Journal of Peptide Science
*J. Peptide Sci.* **4**: 389–399 (1998)

# Conformation and Membrane Activity of an Analogue of the Peptaibol Antibiotic Trichogin GA IV with a Lipophilic Amino Acid at the N-Terminus

**ELSA LOCARDI[a], STEFANO MAMMI[a], EVARISTO PEGGION[a], VANIA MONACO[a], FERNANDO FORMAGGIO[a], MARCO CRISMA[a], CLAUDIO TONIOLO[a,*], BERNARD BODO[b], SYLVIE REBUFFAT[b], JOHAN KAMPHUIS[c] and QUIRINUS B. BROXTERMAN[d]**

[a] Biopolymer Research Center, C.N.R., University of Padova, Department of Organic Chemistry, Padova, Italy
[b] Laboratoire de Chimie, URA 401 CNRS, Muséum National d'Histoire Naturelle, Paris, France
[c] DSM Fine Chemicals, Heerlen, The Netherlands
[d] DSM Research, Organic Chemistry and Biotechnology Section, Geleen, The Netherlands

*Received 9 January 1998*
*Accepted 2 March 1998*

Abstract: We have synthesized by solution-phase methods two analogues of the 11-residue lipopeptaibol antibiotic trichogin GA IV in which the N-terminal *n*-octanoyl group is replaced either by an N-acetylated 2-amino-2-methyl-L-undecanoic acid or by an N-acetylated $\alpha$-aminoisobutyric acid. CD, FTIR absorption, and NMR analyses unequivocally show that the main structural features of trichogin GA IV are preserved in these analogues. Since only the peptide containing the lipophilic chain exhibits membrane-modifying properties, these results strongly support the view that moving the long acyl moiety from the $N^{\alpha}$-blocking group to the side chain of the N-terminal extra-residue does not affect the conformational properties or the membrane activity of trichogin GA IV. © 1998 European Peptide Society and John Wiley & Sons, Ltd.

Keywords: conformational analysis; lipo-amino acid; membrane activity; NMR; peptide antibiotic

## INTRODUCTION

Trichogin GA IV, isolated from *Trichoderma longibrachiatum* and sequenced by Bodo and coworkers [1], is a member of a family of unusual linear peptides exibiting membrane-modifying properties. These compounds are referred to as *lipopeptaibols*, a term that fully describes their chemical structure. Trichogin GA IV is an Aib-rich peptide with the N-terminus acylated by an *n*-Oct group and an L-Lol residue at the C-terminus. The sequence of trichogin GA IV is the following:

$$\overset{1}{n\text{-Oct}}\text{-Aib-Gly-Leu-Aib-}\overset{5}{\text{Gly}}\text{-Gly-Leu-Aib-Gly-}\overset{10}{\text{Ile}}\text{-Lol}$$

We have recently demonstrated that trichogin GA IV and its [L-Leu-$OMe^{11}$] analogue are amphipathic, right-handed, $3_{10}/\alpha$-helical peptides [1–4]. In these lipopeptides, a $N^{\alpha}$-blocking fatty acyl moiety of at least six carbon atoms is required for the onset of significant membrane activity [3]. In an NMR investigation in an aqueous solution containing SDS micelles we have shown that the acyl chain interacts intramolecularly with the first four amino acid residues [4]. In all these investigations the role of the N-terminal lipidic chain has clearly emerged. In order to help our understanding of the require-

Abbreviations: Ac, acetyl; Aib, $\alpha$-aminoisobutyric acid; ($\alpha$Me)Aun, 2-amino-2-methyl-undecanoic acid; CF, carboxyfluorescein; DQF-COSY, double quantum filtered correlation spectroscopy; EDC, N-ethyl-N′-[3-(dimethylamino)propyl]carbodiimide; HFIP, 1,1,1,3,3,3-hexafluoropropan-2-ol; Lol, leucinol; NOESY, nuclear Overhauser effect spectroscopy; Oct, octanoyl; OMe, methoxy; PC, phosphatidylcholine; rmsd, root mean square deviation; SDS, sodium dodecylsulphate; TFA, trifluoroacetic acid; TFE, 2,2,2-trifluoroethanol; TOCSY, total correlation spectroscopy; Z, benzyloxycarbonyl.

* Correspondence to: Biopolymer Research Center, C.N.R., University of Padova, Department of Organic Chemistry, Via Marzolo 1, 35131 Padova, Italy.


CCC 1075–2617/98/060389-11$17.50

ments for the orientation of the acyl chain relative to the peptide backbone, we have synthesized [Ac-L-(αMe)Aun$^0$, L-Leu-OMe$^{11}$] trichogin GA IV, an analogue in which the *n*-octanoyl group is replaced by the new N-acetylated, $C^\alpha$-tetrasubstituted α-amino acid L-(αMe)Aun, characterized by a long hydrocarbon side chain (nine carbon atoms). With the aim at confirming the role of the long acyl chain, we have also prepared the [Ac-Aib$^0$, L-Leu-OMe$^{11}$] trichogin GA IV analogue. This article describes synthesis, characterization, conformational analysis (by CD, FTIR absorption, and NMR techniques), and membrane-modifying properties of these new trichogin GA IV analogues. A preliminary account of part of this work has been reported [5].

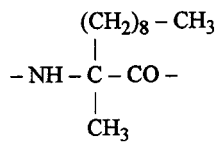

(αMe)Aun

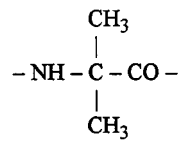

Aib

## MATERIALS AND METHODS

### Peptide Synthesis

Melting points were determined using a Leitz (Wetzlar, Germany) model Laborlux 12 apparatus and are not corrected. Optical rotations were measured using a Perkin-Elmer (Norwalk, CT) model 241 polarimeter equipped with a Haake (Karlsruhe, Germany) model D thermostat. Thin-layer chromatography was performed on Merck (Darmstadt, Germany) Kieselgel 60-$F_{254}$ precoated plates using the following solvent systems: (I) $CHCl_3$/EtOH, 9:1; (II) *n*BuOH/AcOH/$H_2O$, 3:1:1; (III) toluene/EtOH, 7:1. The chromatograms were developed by quenching of UV fluorescence, chlorine–starch–potassium iodide or ninhydrin chromatic reaction as appropriate. All the new compounds were obtained in a chromatographically homogeneous state. The amino acid analyses were performed on a Carlo Erba (Rodano, Milan, Italy) model 3A 30 amino acid analyser. The Aib colour yield with ninhydrin is about 20 times lower than those of protein amino acids. Elution of Aib was observed immediately after the Ala peak. Analytical HPLC was performed on a Pharmacia (Uppsala, Sweden) model LKB-LCC 2252 liquid chromatograph equipped with an UVICORD model SD W detector (226 nm) and a reversed-phase $C_{18}$ Vydac (Hesperia, CA) model 218 TP54 column. MALDI mass spectra were obtained in the positive linear mode at 15 keV acceleration voltage on a Reflex time of flight mass spectrometer (Bruker, Karlsruhe, Germany), using 2,5-dihydroxybenzoic acid as the matrix.

***H-L-(αMe)Aun-OH.*** M.p. 255–256°C; $R_F$(II) 0.75; $[\alpha]^{20}_{546}$ 9.0 (*c* 0.5, MeOH); IR (KBr) 3381, 1642, 1592, 1557 $cm^{-1}$.

***Z-L-(αMe)Aun-OH.*** This compound was prepared from the free amino acid and Z-Cl in a 2M NaOH/acetone mixture (pH 10.8–10.9): yield: 82%; oil; $R_F$(I) 0.75, $R_F$(II) 0.90, $R_F$(III) 0.50; $[\alpha]^{20}_D$ 4.9 (*c* 0.5, EtOAc); IR (KBr): 3417, 3332, 1709 $cm^{-1}$; $^1$H NMR (200 MHz, $CDCl_3$) δ (ppm) 9.65 (broad, 1H, COOH OH), 7.36 (m, 5H, Z phenyl CH), 5.53 [s, 1H, (αMe)Aun NH], 5.09 (s, 2H, Z $CH_2$), 2.10 and 1.80 [2m, 2H, (αMe)Aun β$CH_2$], 1.60 [s, 3H, (αMe)Aun β$CH_3$], 1.24 [m, 14H, (αMe)Aun $(CH_2)_7$], 0.87 [t, 3H, (αMe)Aun ω$CH_3$].

***[Z-L-(αMe)Aun]$_2$O.*** This compound was synthesized from Z-L-(αMe)Aun-OH and EDC hydrochloride in a 2:1 molar ratio in anhydrous $CH_3CN$. The crude product was purified by flash chromatography (silica gel column; eluant EtOAc-light petroleum 1:7): yield 65%; oil; $[\alpha]^{20}_D$ 1.0 (*c* 0.6, EtOAc); $[\alpha]^{20}_{365}$ 4.5 (*c* 0.6, EtOAc); IR (KBr) 3405, 3339, 1818, 1718, 1586 $cm^{-1}$; 1H NMR (250 MHz, $CDCl_3$) δ (ppm) 7.33 (m, 10H, Z phenyl CH), 5.20 [s, 2H, (αMe)Aun NH], 5.07 (s, 4H, Z $CH_2$), 1.90 and 1.70 [2m, 4H, (αMe)Aun β$CH_2$], 1.52 [s, 6H, (αMe)Aun β$CH_3$], 1.26 [m, 28H, (αMe)Aun $(CH_2)_7$], 0.87 [t, 6H, (αMe)Aun ω$CH_3$].

***Z-L-(αMe)Aun-Aib-Gly-L-Leu-Aib-Gly$_2$-L-Leu-Aib-Gly-L-Ile-L-Leu-OMe.*** This compound was prepared from the $N^\alpha$-deprotected C-terminal undecapeptide, obtained by catalytic hydrogenolysis of the corresponding Z-derivative [3] in MeOH solution, and [Z-L-(αMe)Aun]$_2$O in anhydrous $CH_3CN$ in the presence of NMM. The crude product was purified by flash chromatography (silica gel column; eluant $CHCl_3$-EtOH 91:9): yield 62%; m.p. 114–116°C; $R_F$(I) 0.45, $R_F$(II) 0.85, $R_F$(III) 0.95; $[\alpha]^{20}_D$ −8.1 (*c* 0.5, MeOH); amino acid analysis: Aib 3.01, Gly 4.04, Ile 0.95, Leu 3.01; IR (KBr): 3323, 1739, 1658, 1538 $cm^{-1}$; 1H NMR (250 MHz, $CDCl_3$) δ (ppm) 8.13 (t, 1H, Gly NH, 7.75 (m, 3H, 3 NH), 7.52 (m, 4H, Ile NH, 3 NH), 7.45 (s, 1H, Aib NH), 7.35 (m, 5H, Z phenyl CH), 7.25 (d, 1H, Leu NH), 7.15 (s, 1H, Aib NH), 6.15 [s, 1H, (αMe)Aun NH], 5.10 (m, 2H, Z

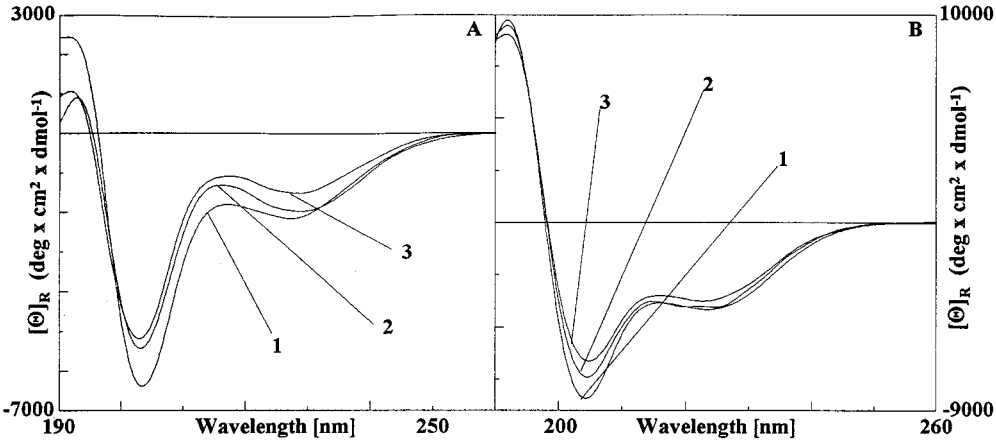


Figure 1 CD spectra of [Ac-L-(αMe)Aun$^{0}$, L-Leu-OMe$^{11}$] trichogin GA IV (1), [L-Leu-OMe$^{11}$] trichogin GA IV (2), and [Ac-Aib$^{0}$, L-Leu-OMe$^{11}$] trichogin GA IV (3) 1 mM in MeOH solution (A) and 3 mM in aqueous solution containing 300 mM SDS (B).

$CH_2$), 4.56 (m, 1H, Leu αCH), 4.45 (m, 1H, Ile αCH), 4.15 (m, 2H, 2 Leu αCH), 4.10–3.70 (m, 7H, 4 Gly $\alpha CH_2$), 3.52 (dd, 1H, Gly $\alpha CH_2$), 3.69 (s, 3H, OMe $CH_3$), 2.04 (m, 1H, Ile βCH), 1.90–1.20 [m, 13H, 3 Leu $\beta CH_2$, 3 Leu γCH, Ile $\gamma CH_2$, (αMe)Aun $\beta CH_2$], 1.66, 1.52, 1.47 and 1.43 [4s, 21H, 3 Aib $\beta CH_3$, (αMe)Aun $\beta CH_3$], 1.26 [m, 14H, (αMe)Aun $(CH_2)_7$], 1.05–0.80 [m, 27H, 3 Leu $\delta CH_3$, Ile $\gamma CH_3$, Ile $\delta CH_3$, (αMe)Aun $\omega CH_3$].

***Ac-L-(αMe)Aun-Aib-Gly-L-Leu-Aib-Gly$_2$-L-Leu-Aib-Gly-L-Ile-L-Leu-OMe.*** This compound was synthesized from the peptide described above (after $N^{\alpha}$-deprotection by catalytic hydrogenolysis in MeOH solution) and acetic anhydride. The product was crystallized from EtOAc: yield 85%; m.p. 213–214°C; $R_F$(I) 0.05, $R_F$(II) 0.75, $R_F$(III) 0.95; $[\alpha]_D^{20} -$ 18.0 (*c* 0.5, MeOH); amino acid analysis: Aib 2.85, Gly 4.10, Ile 0.97, Leu 3.10; IR (KBr): 3312, 1742, 1655, 1539 $cm^{-1}$; 1H NMR (400 MHz, $CDCl_3$) δ(ppm) 8.22 (m, 1H, NH), 8.16 (m, 1H, NH), 8.02 (m, 1H, NH), 7.90 (m, 1H, NH), 7.87 (m, 1H, NH), 7.79 (m, 1H, NH), 7.67 (m, 1H, NH), 7.66 – 7.52 (m, 4H, 4 NH), 7.51 (m, 1H, NH), 4.51 (m, 1H, Leu αCH), 4.32 (m, 1H, Ile αCH), 4.11 (m, 3H, 2 Leu αCH, Gly $\alpha CH_2$), 4.05 – 3.60 (m, 7H, 4 Gly $\alpha CH_2$), 3.72 (s, 3H, OMe $CH_3$), 2.04 (m, 1H, Ile βCH), 2.02 (s, 3H, Ac $CH_3$), 1.90 – 1.60 [m, 12H, 3 Leu $\beta CH_2$, 3 Leu γCH, (αMe)Aun $\beta CH_2$, Ile $\gamma CH_2$], 1.59, 1.55, 1.54, 1.51, 1.45 and 1.42 [6s, 21H, 3 Aib $\beta CH_3$, (αMe)Aun $\beta CH_3$], 1.40 – 1.20 [m, 15H, (αMe)Aun $(CH_2)_7$, Ile $\gamma CH_2$], 1.00 – 0.80 [m, 27H, 3 Leu $\delta CH_3$, Ile $\gamma CH_3$, Ile $\delta CH_3$, (αMe)Aun $\omega CH_3$]. MALDI-MS (MW 1206): *m/z* 1231 $[(M + Na)^+]$.

***Z-Aib$_2$-Gly-L-Leu-Aib-Gly$_2$-L-Leu-Aib-Gly-L-Ile-L-Leu-OMe.*** This compound was prepared from the $N^{\alpha}$-deprotected C-terminal undecapeptide, obtained by catalytic hydrogenolysis of the corresponding Z-derivative [3] in MeOH solution, and $(Z\text{-Aib})_2O$ [6,7] in anhydrous $CH_3CN$ in the presence of NMM. The product was crystallized from EtOAc-light petroleum: yield 85%; m.p. 143–145°C; $R_F$(I) 0.30, $R_F$(II) 0.85, $R_F$(III) 0.95; $[\alpha]_D^{20} -$ 10.9 (*c* 0.5, MeOH); amino acid analysis: Aib 4.23, Gly 4.02, Ile 0.98, Leu 3.01; IR (KBr) 3322, 1738, 1659, 1536 $cm^{-1}$; 1H NMR (250 MHz, $CDCl_3$) δ (ppm) 8.10 (broad t, 1H, Gly NH), 7.81 (broad t, 1H, Gly NH), 7.70 (m, 2H, 2 NH), 7.60 (m, 1H, Ile NH), 7.54 (m, 4H, 4 NH), 7.44 (s, 1H, Aib NH), 7.40 – 7.30 (m, 1H, 1 NH), 7.33 (m, 5H, Z phenyl CH), 6.79 (s, 1H, Aib NH), 5.09 (m, 2H, Z $CH_2$), 4.56 (m, 1H, Leu αCH), 4.40 (m, 1H, Ile αCH), 4.20 – 3.70 (m, 9H, 2 Leu αCH, 4 Gly $\alpha CH_2$), 3.67 (s, 3H, OMe $CH_3$), 3.49 (dd, 1H, Gly $\alpha CH_2$), 2.02 (m, 1H, Ile, βCH), 1.90 – 1.20 (m, 11H, 3 Leu $\beta CH_2$, 3 Leu γCH, Ile $\gamma CH_2$), 1.52 (1s, 12H, 2 Aib $\beta CH_3$), 1.45 (1s, 6H, Aib $\beta CH_3$), 1.41 and 1.29 (2s, 6H, Aib $\delta CH_3$), 1.00 – 0.80 (m, 24H, 3 Leu $\delta CH_3$, Ile $\gamma CH_3$, Ile $\delta CH_3$).

***Ac-Aib$_2$-Gly-L-Leu-Aib-Gly$_2$-L-Leu-Aib-Gly-L-Ile-L-Leu-OMe.*** This compound was synthesized from the peptide described above (after $N^{\alpha}$-deprotection by catalytic hydrogenolysis in MeOH solution) and acetic anhydride. The crude product was purified by preparative HPLC [eluant: A = 0.05% TFA in water; B = 0.05% TFA in a 9:1 $CH_3CN$–water mixture; isocratic elusion: 60% B for 30 min; flux: 5 ml/min; column: reverse phase $C_{18}$ Vydac Model 218

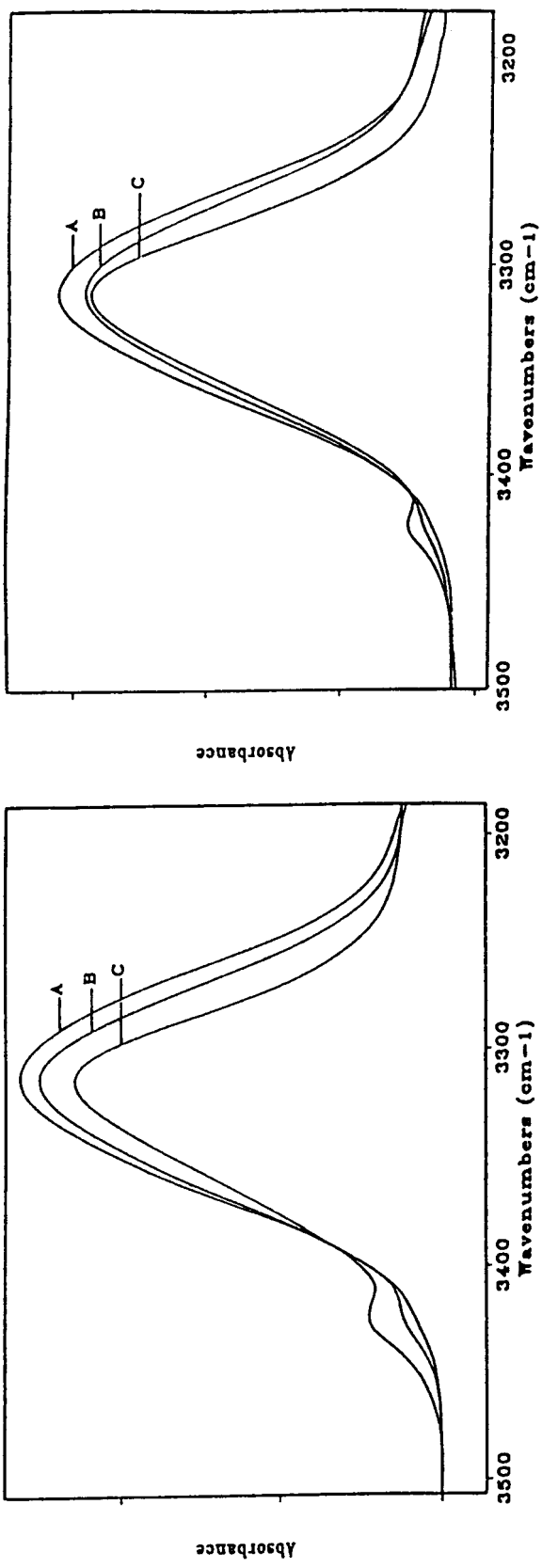


Figure 2 FTIR absorption spectra of [Ac-L-(αMe)Aun$^0$, L-Leu-OMe$^{11}$] trichogin GA IV (left panel) and [Ac-Aib$^0$, L-Leu-OMe$^{11}$] trichogin GA IV (right panel) in $CDCl_3$ solution: curve A, 10 mM concentration; curve B, 1 mM concentration; curve C, 0.1 mM concentration.

Table 1 Proton Chemical Shift Values (ppm) at 298 K Relative to Tetramethylsilane and Temperature Dependence of the Amide Proton Chemical Shift Values (ppb/K) for [Ac-L-(αMe)Aun$^{0}$, L-Leu-OMe$^{11}$] Trichogin GA IV in Aqueous Solution in the Presence of 300 mM SDS

| Residue | NH ($-\Delta\delta/\Delta T$) | αCH | βCH | Other H |
|---|---|---|---|---|
| Ac | | | | $CH_3$ 2.19 |
| Aun 0 | 8.32 (6.5 ± 0.3) | | $CH_3$ 1.50; $CH_2$ ~ 1.89 | $(CH_2)_7$ 1.40 – 1.32; ω$CH_3$ 0.92 |
| Aib 1 | 8.44 (5.6 ± 0.4) | | 1.56 | |
| Gly 2 | 8.14 (2.4 ± 0.2) | 4.08/4.02 | | |
| Leu 3 | 8.12 (2.3 ± 0.3) | 4.47 | ~ 1.89/1.77 | γCH ~ 1.89; δ$CH_3$ 1.02/1.01 |
| Aib 4 | 7.85 (2.5 ± 0.3) | | 1.64/1.56 | |
| Gly 5 | 8.54 (6.9 ± 0.5) | 4.06/3.98 | | |
| Gly 6 | 8.33 (3.6 ± 0.7) | 4.19/3.98 | | |
| Leu 7 | 7.94 (3.2 ± 0.5) | 4.33 | ~ 1.84 | γCH ~ 1.84; δ$CH_3$ 1.02 |
| Aib 8 | 8.06 (5.4 ± 0.2) | | 1.62/1.57 | |
| Gly 9 | 7.96 (3.2 ± 0.4) | 4.14/3.95 | | |
| Ile 10 | 7.91 (2.2 ± 0.3) | 4.36 | 2.11 | γ$CH_2$ 1.70/1.46; γ$CH_3$ 1.07; δ$CH_3$ 1.00 |
| Leu 11 | 7.52 (2.1 ± 0.4) | 4.55 | ~ 1.86/1.74 | γCH ~ 1.86; δ$CH_3$ ~ 1.01 |
| OMe | | | | $CH_3$ 3.88 |

TP1022]: yield 62%; m.p. 182–183°C; $R_F$(II) 0.70, $R_F$(III) 0.90; $[\alpha]_D^{20} - 16.3$ (*c* 0.3, MeOH); amino acid analysis: Aib 4.17, Gly 3.75, Ile 0.98, Leu 3.09; IR (KBr) 3311, 1742, 1659, 1538 $cm^{-1}$; $^1H$ NMR (400 MHz, $CDCl_3$) δ (ppm) 8.20 (m, 4H, 4 NH), 7.90 (m, 1H, 1 NH), 7.86 (m, 1H, 1 NH), 7.75 (m, 4H, 4 NH), 7.61 (m, 1H, 1 NH), 7.49 (m, 1H, 1 NH), 4.53 (m, 1H, Leu αCH), 4.26 (m, 1H, Ile αCH), 4.10 (m, 3H, 2 Leu αCH, Gly α$CH_2$), 4.00 – 3.70 (m, 7H, 4 Gly α$CH_2$), 3.73 (s, 3H, OMe $CH_3$), 2.02 (m, 1H, Ile βCH), 2.02 (s, 3H, Ac $CH_3$), 1.90 – 1.60 (m, 10H, 3 Leu β$CH_2$, 3 Leu γCH, Ile γ$CH_2$), 1.56, 1.55, 1.54, 1.53, 1.49, 1.48, 1.46 and 1.45 (8s, 24H, 4 Aib β$CH_3$), 1.33 (m, 1H, Ile γ$CH_2$), 1.05 – 0.80 (m, 24H, 3 Leu δ$CH_3$, Ile γ$CH_3$, Ile δ$CH_3$). MALDI-MS (MW 1094): *m*/*z* 1097 [$(M + H)^+$], 1118 [$(M + Na)^+$], 1133 [$(M + K)^+$].

### Liposome Leakage Assay

Peptide-induced leakage from egg PC vesicles was measured at 20°C using the CF-entrapped vesicle technique as previously described [8]. CF-encapsulated small unilamellar vesicles (egg PC/cholesterol, 7:3) were prepared by sonication in Hepes buffer, pH 7.4. The phospholipid concentration was kept constant (0.6 mM), and increasing [peptide]/[lipid] molar ratios ($R_i^{-1}$) were obtained by adding aliquots of methanolic solutions of peptides, keeping the final methanol concentration below 5% by volume. After rapid and vigorous stirring, the time course of fluorescence change corresponding to CF escape was recorded at 520 nm (1 nm band pass) with $\lambda_{exc}$ 488 nm (1 nm band pass). The percentage of released CF at time *t* was determined as $(F_t - F_o)/(F_T - F_o) \times 100$, with $F_0$, fluorescence intensity of vesicles in the absence of peptide; $F_t$, fluorescence intensity at time *t* in the presence of peptide; and $F_T$, total fluorescence intensity determined by disrupting the vesicles by addition of 30 μl of a 10% Triton X-100 solution. The kinetics were stopped at 20 min.

### FTIR Absorption

The solution FTIR absorption spectra were recorded using a Perkin-Elmer Model 1720X FTIR spectrophotometer, nitrogen-flushed, equipped with a sample-shuttle device, at 2 $cm^{-1}$ nominal resolution, averaging 100 scans. Solvent (baseline) spectra were obtained under the same conditions. Cells with path lengths of 0.1, 1.0, and 10 mm (with $CaF_2$ windows) were used. Spectrograde deuterochloroform (99.8% *d*) was purchased from Fluka (Buchs, Switzerland). The solid-state IR absorption measurements were performed using the KBr disk technique and a Perkin-Elmer model 580 B spectrophotometer equipped with a Perkin-Elmer model 3600 data station.

### Circular Dichroism

The CD spectra were obtained on a Jasco (Hachioji City, Japan) model J-710 spectropolarimeter. Cylindrical fused quartz cells of 10, 1, 0.2, and 0.1 mm

path lengths (Hellma, Mullheim/Baden, Germany) were used. The values are expressed in terms of $[\Theta]_R$, the residue molar ellipticity (deg·cm$^2$·dmol$^{-1}$). Spectrograde MeOH and EtOH (Baker, Deventer, The Netherlands), and TFE and HFIP (Acros, Geel, Belgium) were used as solvents.

### NMR Spectroscopy

Two-dimensional NMR spectra were recorded on a Bruker AM 400 spectrometer at 298 K. The data were processed on a Bruker X-32 workstation. The NMR sample contained 3 mM peptide in 90% $H_2O$/10% $D_2O$ in the presence of 0.3 M SDS-$d_{25}$ (CIL, Andover, MA). The pH of the solution was *ca.* 5

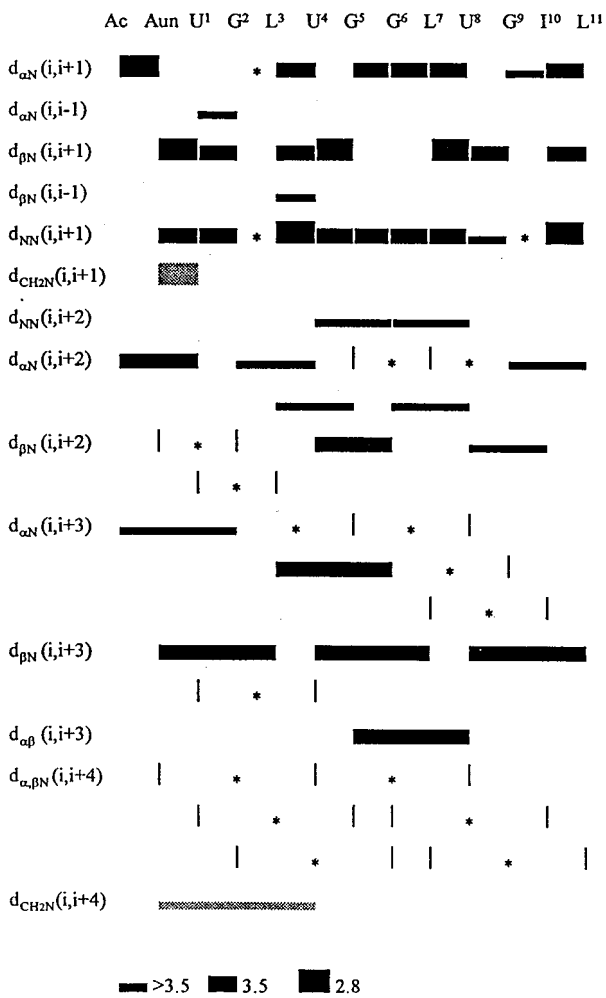


Figure 3 Interresidue NOE's found for [Ac-L-(αMe)Aun$^0$, L-Leu-OMe$^{11}$] trichogin GA IV in aqueous solution containing SDS micelles. Asterisks indicate the likely presence of a peak obscured by overlap. A grey motif indicates that it was not possible to determine how many protons are involved in the peak. U, Aib.

(uncorrected). Homonuclear 2D-NMR spectra were acquired in the phase sensitive mode using the time proportional phase increment method [9,10]. Quadrature detection was used in both dimensions. The water signal was suppressed by pre-irradiation with a selective gated pulse during the relaxation delay and in the case of NOESY also during the mixing time. The carrier frequency was placed at the frequency of the water resonance and the saturating RF was phase-coherent with the receiver. At the beginning of each transient, a homospoil pulse was applied in order to destroy residual transverse magnetization. Depending on the experiment sensitivity, a variable number of scans between 256 and 320 was acquired for each $t_1$ increment; 350 to 400 $t_1$ increments were typically collected, of 2K data points each. Free induction decays were multiplied by appropriate windows functions in both time domains and zero filled to 2K × 1K real points. The clean-TOCSY [11] spectrum was acquired with 75 ms of MLEV-17 isotropic mixing, including two trim pulses of 2.5 ms each and 'cleaning' delays equal to twice the length of the 90° pulse in the spin-locking sequence. A spin-locking field of $\gamma B_2/2\pi = 5$ kHz was applied. The two-dimensional NOESY [12] spectrum was carried out with 200 ms mixing time. A 10% random variation of the mixing period was applied to eliminate ZQ coherence contributions [13]. 1D-NMR spectra were recorded in the temperature range between 298 and 320 K in order to determine the temperature dependence of the amide proton resonances.

Cross peak volumes in the NOESY spectrum were integrated using the AURELIA software. The values thus obtained were converted into interproton distances using fixed geometrical distances or standard distances in regular secondary structures. As reference, the distance of 1.78 Å for the Ile$^{10}$ $\gamma_1/\gamma_2$ was used in the aliphatic region of the NOESY spectrum. The amide region was calibrated on the sequential distance between the NH protons of Leu$^3$ and Aib$^4$ (2.6 Å in the $3_{10}$-helix) on the basis of the high helix content found at this point of the sequence. All the resulting values were then classified in six classes with cut off limits of 2.8, 3.2, 3.5, 4.0, 5.0 and 6.0 Å, respectively, and used as upper limits in the estimation of the three-dimensional structure of the peptide by means of distance geometry and molecular dynamics protocols.

### Structure Calculations

A set of 50 different initial random structures satisfying the experimental restraints were generated by

distance geometry calculations using the program DIANA version 2.1 [14] running on a Digital AXP computer. Lower limits on interproton distances were set according to the sum of van der Waals radii. The strategy employed involves a gradual introduction of the NOE restraints and the increase of the weight of the van der Waals contacts only at the end of simulation. Energy minimization and simulated annealing calculations were both carried out using the software package X-PLOR version 3.2 [15]. A harmonic repulsive potential of the form $V_{vdw} = k_{vdw}(s^2 r_{min}^2 - r^2)^2$ was used for nonbonded interaction, introducing the sum of van der Waals radii as minimum distances. NOE restraints were taken into account by means of a double harmonic potential, utilizing them as upper limits of interproton distances. A potential of the form $V_{NOE} = a + b/\Delta + c \cdot \Delta$ was used in the case of violations greater than 0.5 Å. Lower limits were set to 1.8 Å for all values. All the calculations were performed *in vacuo*. The distance geometry structures were refined to reach the lowest penalty value using at first 2200 steps of the steepest descent minimization method, using a low force constant for both nonbonded and NOE interactions, to remove internal strain and improve the covalent geometry of the system. Such a minimization results in a local minimum structure. A simulating annealing protocol was then applied in order to enable the system to get out of local minima. It involves high temperature heating followed by slow cooling to overcome potential barriers along the pathway towards the global minimum region. Several cycles of the following protocol were applied to each structure: (i) 5 ps of dynamics at 1000 K, using 5 fs steps with $k_{NOE} = 30$ kcal·mol$^{-1}$·Å$^{-2}$, $k_{vdw} = 0.002$ kcal·mol$^{-1}$·Å$^{-2}$, $c = 0.1$ and $s = 1$. Weights of the bond and improper angles were 0.4 and 0.1, respectively; (ii) 5 ps of dynamics at 1000 K, using 2 fs steps. The constant forces were not changed, while the asinthotic coefficient $c$ reached the value of 1. In order to fix the geometry of the system also bond and improper angle terms were increased to 1; (iii) the system was cooled down to 200 K in steps of 50 K, for a total time of 7.14 ps. During this time, weights relative to NOE and van der Waals interactions were increased by slowly increasing the values of $k_{NOE}$ and $k_{vdw}$ to 60 kcal·mol$^{-1}$·Å$^{-2}$ and to 4 kcal·mol$^{-1}$·Å$^{-2}$, respectively. The repulsive term $s$ was decreased from 1 to 0.75; (iv) 300 steps of energy minimization, leaving the parameters of the energy terms unmodified, to ensure the best geometry. The final structures were displayed using the software Insight II (Biosym Technologies Inc., San Diego, CA) on a Silicon Graphics (Mountain View, CA) Iris workstation.

## RESULTS AND DISCUSSION

### Peptide Synthesis and Characterization

For the large-scale production of the enantiomerically pure L-(αMe)Aun we exploited an economically attractive and generically applicable chemo-enzymatic synthesis developed by DSM Research (Geleen, The Netherlands) [16,17] a few years ago. It involves a combination of organic synthesis for the preparation of the racemic α-amino acid amide followed by the use of a broadly specific amino acid amidase to achieve optical resolution.

The [Ac-L-(αMe)Aun$^0$, L-Leu-OMe$^{11}$] and [Ac-Aib$^0$, L-Leu-OMe$^{11}$] analogues were synthesized from H-Aib-Gly-L-Leu-Aib-Gly$_2$-L-Leu-Aib-Gly-L-Ile-L-Leu-OMe [prepared, in turn, from the Z-protected synthetic precursor [3] by catalytic hydrogenation] and the Z-protected symmetrical anhydride either from L-(αMe)Aun or Aib [6,7], followed by N$^\alpha$-deprotection and acetylation with acetic anhydride. The intermediates and the final products were extensively purified and characterized by chromatographic techniques, polarimetry, amino acid analysis, solid-state IR absorption, $^1$H NMR, and mass spectrometry.

### Conformational Analysis

The CD spectra of [L-Leu-OMe$^{11}$] trichogin GA IV and the two N$^\alpha$-modified [Ac-L-(αMe)Aun$^0$, L-Leu-OMe$^{11}$] and [Ac-Aib$^0$, L-Leu-OMe$^{11}$] analogues in a variety of organic solvents (MeOH, EtOH, TFE, and HFIP), as well as in water in the presence of SDS micelles have a similar shape, showing a negative maximum (peptide $\pi \rightarrow \pi^*$ exciton split band) [18] in the range 202–205 nm and a negative, broad and weaker shoulder (peptide $n \rightarrow \pi^*$ transition) centred at about 220 nm (as representative examples, Figure 1 shows the CD spectra in MeOH and in SDS micelles). In SDS micelles, the intensity of the long-wavelength shoulder is more pronounced. Concurrently, the conformationally sensitive ratio $R = [\Theta]_{222}/[\Theta]_{208}$ [19] changes from 0.25–0.35 (in the alcohols) to about 0.50 (in SDS micelles). We interpret these CD spectra as arising from a contribution of (right-handed) mixed $3_{10}/\alpha$-helical conformations with increased α-helix population in SDS micelles

Table 2 Distribution of the NOE Peaks Detected in Aqueous Solution in the Presence of 300 mM SDS and Average Backbone Torsion Angles (°) for the Minimized Structures of [Ac-L-(αMe)Aun$^0$, L-Leu-OMe$^{11}$] Trichogin GA IV. The Number of Structures over Which the Average Was Taken Is Indicated in Brackets

| Residue | Intraresidue | Sequential | Medium-range | Φ | Ψ | |
|---|---|---|---|---|---|---|
| Ac | – | 1 | 3 | | | |
| Aun 0 | 2 | 3 | 1 | – | – | |
| Aib 1 | 2 | 5 | 1 | $-173 \pm 5$ | $42 \pm 11$ | [13] |
| Gly 2 | 0 | 3 | 2 | $-102 \pm 16$ | $-14 \pm 26$ | [10] |
| Leu 3 | 10 | 5 | 4 | $-94 \pm 14$ | $-29 \pm 9$ | [25] |
| Aib 4 | 4 | 8 | 5 | $-65 \pm 5$ | $-29 \pm 15$ | [29] |
| Gly 5 | 6 | 5 | 3 | $-62 \pm 12$ | $-12 \pm 14$ | [29] |
| Gly 6 | 2 | 5 | 6 | $-56 \pm 10$ | $-44 \pm 6$ | [27] |
| Leu 7 | 6 | 6 | 4 | $-92 \pm 11$ | $0 \pm 22$ | [26] |
| Aib 8 | 4 | 5 | 6 | $-54 \pm 12$ | $-56 \pm 23$ | [28] |
| Gly 9 | 4 | 4 | 2 | $-74 \pm 18$ | $-26 \pm 11$ | [28] |
| Ile 10 | 28 | 8 | 4 | $-51 \pm 4$ | $-27 \pm 5$ | [31] |
| Leu 11 | 10 | 6 | 3 | – | – | |

[19]. Despite differences in the sequence of the N-terminal part, the CD spectra and the contributing conformational preferences of the three peptides seem to be quite comparable.

The FTIR absorption spectra of the three undecapeptide esters (for two examples, see Figure 2) in the most informative N–H stretching region (3500–3200 cm$^{-1}$) in $CDCl_3$ are dominated by a strong and broad band at 3325–3310 cm$^{-1}$ (H-bonded NH groups) [20,21]. An additional, extremely weak band (shoulder) is seen at 3430–3420 cm$^{-1}$ (free, solvated NH groups). This spectral pattern is typical of highly H-bonded, helical peptides [22]. Between 10 and 0.1 mM concentration, a distinct spectral change is observed (Figure 2), indicative of the contribution of a significant amount of intermolecular H-bonds. Self-association is less evident in the [Ac-Aib$^0$, L-Leu-OMe$^{11}$] analogue, which lacks the N-terminal lipophilic moiety. In any case, at the lowest concentration examined (0.1 mM) the 3325–3310 cm$^{-1}$ band is still very intense in all three analogues, supporting the view that these peptides are characterized by an intense set of intramolecular C = O···H–N H-bonds.

The $^1$H-NMR spectrum of [Ac-L-(αMe)Aun$^0$, L-Leu-OMe$^{11}$] trichogin GA IV in aqueous solution containing SDS micelles was assigned with the standard two-dimensional techniques DQF-COSY, TOCSY and NOESY. The chemical shifts of the assigned peaks are reported in Table 1. With the DQF-COSY and TOCSY experiments all the spin systems were identified with the exception of those of the Aib residues because of the lack of any scalar correlation between the methyl groups and the amide proton. The NOESY spectrum allowed for the unambiguous assignment of all the residues in the sequence through $d_{\alpha N}$ and $d_{\beta N}$ sequential connectivities. The NOE data are summarized in Figure 3 and in Table 2. The presence of sequential $d_{NN}$ and medium range $i \rightarrow i+2$, $i \rightarrow i+3$ correlations throughout the sequence is a clear evidence that the peptide folds into a helical structure. More specifically, $i \rightarrow i+2$ proximities are more characteristic of $3_{10}$-helical stretches. On the other hand, fairly intense $d_{\alpha N}$ cross-peaks and a reverse $i \rightarrow i-1$ peak at the N-terminus are also present. Because of the overlap of several resonances the set of NOE data may not be complete. For instance, most of the medium range $i \rightarrow i+4$ connectivities, very important to discriminate between the α-helix and the $3_{10}$-helix, are obscured by overlap, and it is not possible to assign them. The temperature dependence of the NH chemical shifts is linear in the temperature range explored (298–313 K). The values, reported in Table 1, indicate that the N-terminal region is slightly more ordered than that of the [L-Leu-OMe$^{11}$] trichogin analog [4], while no significant differences were detected in the C-terminal region. Interestingly, in both peptides the same high temperature coefficient ($-\Delta\delta/\Delta T$) was observed for both Gly$^5$ and Aib$^8$ NH's, thereby excluding the presence of a continuous helical folding.

Only 31 out of the 50 best structures generated by DIANA were successfully minimized with the simulated annealing protocols (X-PLOR). After re-

finement, they showed an average backbone pairwise rmsd of 1.22 Å for the sequence between residues 4 and 11, with a standard deviation of 0.73 Å (minimum 0.08, maximum 3.07) and none of the structures had NOE restraint violations greater than 0.3 Å. The angles recovered from the dynamics and averaged over the final structures (Table 2) reveal a mixed $\alpha/3_{10}$-helical folding of the peptide. This conformation is present in all the minimized structures starting from residue 4, while the structure of the N-terminus is much less determined (Figure 4). The $\psi$ angle of Leu$^{7}$ is far from helical values and is more consistent with a type I $\beta$-turn centred at Gly$^{6}$-Leu$^{7}$. As can be seen from Table 2, the N-terminal region of the peptide exhibits fewer experimental restraints relative to the rest of the molecule and the definition of its structure is consequently poorer. Since the number of ambiguous peaks was not higher for this region than for the rest of the peptide, this result can be interpreted with a higher flexibility of the N-terminus. Nevertheless, the small number of restraints confined at least a few of the minimized structures into a limited region of the Ramachandran map. In Table 2, the average torsion angles for residues Aib$^{1}$ and Gly$^{2}$ are given for these structures. Clearly, the angles given in Table 2 for these residues are not the only ones compatible with the experimental restraints. Nevertheless, it is significant that partial order starts already at residue 1. On the other hand, the $\psi$ angle of Aun$^{0}$ and the $\phi$ angle of Leu$^{11}$ were dispersed over the whole Ramachandran map.

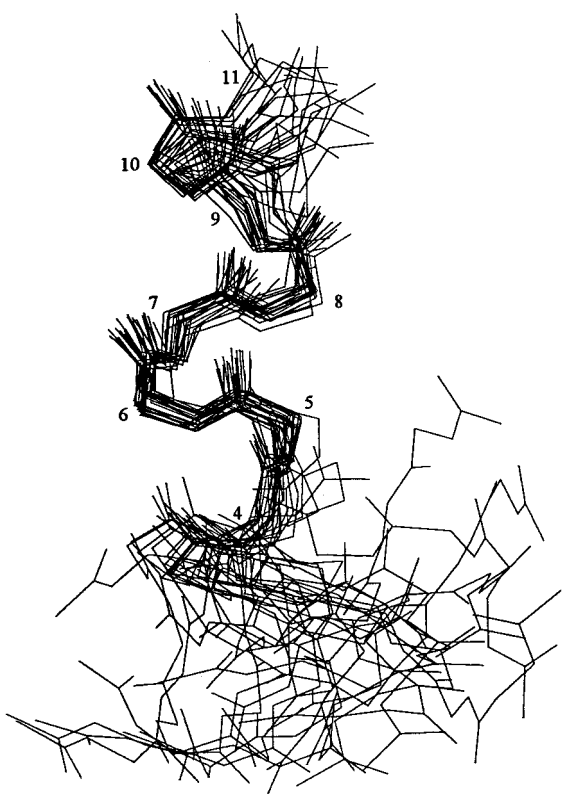


Figure 4 Overlap of the sequence 4–11 of 25 structures of [Ac-L-($\alpha$Me)Aun$^{0}$, L-Leu-OMe$^{11}$] trichogin GA IV selected among the 31 minimized structures.

In the minimized structures, stable intramolecular H-bonds were found between Gly$^{6}$ (NH) and Leu$^{3}$ (CO), as well as between Leu$^{11}$ (NH) and Aib$^{8}$ (CO), defining the beginning and the end of the helix as $3_{10}$ (Figure 4). The amide protons of residues between 7 and 10 are involved in mixed H–bond patterns. Leu$^{7}$ (NH) displays mainly $C_{10}$ structures, while Gly$^{9}$ (NH) and Ile$^{10}$ (NH) prefer (distorted) $C_{13}$ arrangements. The amide proton of Aib$^{8}$ was seldom involved in H–bonds, in agreement with its high temperature coefficient.

The main structural features found in other trichogin GA IV analogues [4] are preserved in the present case. However, in the [Ac-L-($\alpha$Me)Aun$^{0}$, L-Leu-OMe$^{11}$] analogue Gly$^{5}$ is less flexible than in [L-Leu-OMe$_{11}$] trichogin GA IV, but this phenomenon could just reflect the higher number of experimental restraints involving this residue. Similar to what found in previous studies [4], some intramolecular NOESY connectivities were detected between the proximal methylene protons in the lipophilic side chain of ($\alpha$Me)Aun$^{0}$ and the amide protons of the first residues up to Aib$^{4}$ (Figure 3).

In a trichogin GA IV analogue where it was possible to define the direction of the N-terminal fatty acyl chain, a perpendicular orientation with respect to the helical axis was found [4].

## Membrane-Modifying Properties

The membrane-modifying properties of the [Ac-L-($\alpha$Me)Aun$^{0}$, L-Leu-OMe$^{11}$] and [Ac-Aib$^{0}$, L-Leu-OMe$^{11}$] trichogin GA IV analogues are compared in Figure 5 with those of the [L-Leu-OMe$^{11}$] analogue and the natural lipopeptaibol (in this assay, the properties of the last two peptides are identical). A very high activity was observed for the [Ac-L-($\alpha$Me)Aun$^{0}$, L-Leu-OMe$^{11}$] analogue, whereas the [Ac-Aib$^{0}$, L-Leu-OMe$^{11}$] analogue lacks any membrane-modifying property. These results confirm our previous data [3] on the essential role played by the fatty acyl chain on the membrane activity of trichogin GA IV. The higher activity exhibited by the [Ac-L-($\alpha$Me)Aun$^{0}$, L-Leu-OMe$^{11}$] analogue compared

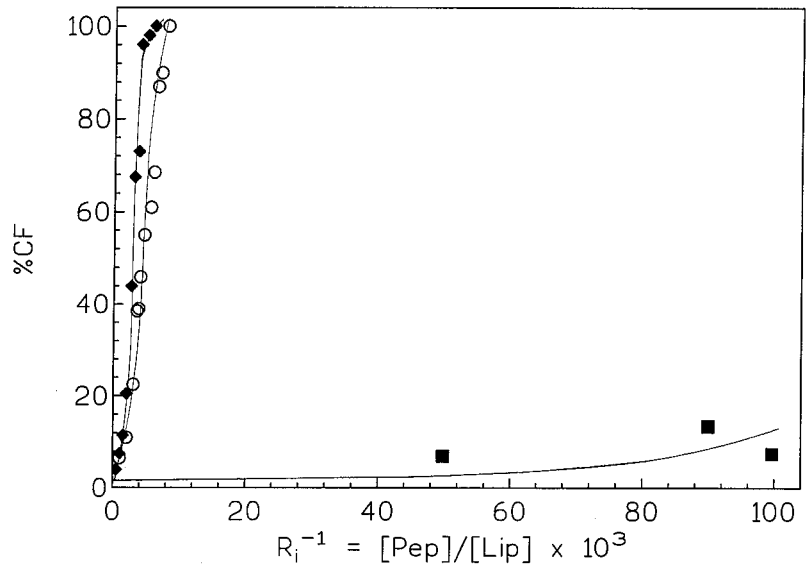


Figure 5 Peptide-induced CF leakage at 20 min for different ratios $R_i^{-1}$ = [peptide]/[lipid] from egg PC/cholesterol (70:30) unilamellar vesicles: ◆, [Ac-L-(αMe)Aun$^0$, L-Leu-OMe$^{11}$] trichogin GA IV; ○, [L-Leu-OMe$^{11}$] trichogin GA IV and trichogin GA IV; ■, [Ac-Aib$^0$, L-Leu-OMe$^{11}$] trichogin GA IV.

with trichogin GA IV itself may well be associated with the higher number of carbon atoms present in the lipophilic chain of the former peptide. In fact, we have already shown [3] that the membrane activity of trichogin GA IV increases with increasing number of carbon atoms in the N$^\alpha$-blocking fatty acyl moiety.

## CONCLUSIONS

A considerable body of evidence has been accumulated in the literature to support the view that the N$^\alpha$-acetylated 15–19 amino acid peptaibols are helical and capable of forming channels in biological membranes through which water molecules and ions may readily pass [23]. For these long peptaibols the helix length is sufficient to span the lipid bilayer. In contrast, the helix length of trichogin GA IV [2] is approximately half that of alamethicin. It is reasonable to conclude that, if the mechanism of action for this latter class of peptaibols (short lipopeptaibols) involves channel formation in bilayers, the arrangement of molecules required to bring about such disruptions must be quite different from the longer N$^\alpha$-acetylated sequences. Noncovalent linkage of two trichogin molecules ('dimer' formation) at the membrane surface via the orthogonally-oriented fatty acyl chains covalently bound to the α-amino groups, and subsequent insertion into the membrane, could lead to a molecular aggregate with Gly-rich faces at its interior to generate a hydrophilic channel of sufficient length to span the bilayer. However, it should be pointed out that the orientation of a peptide in the liposome lipid is not necessarily the same as in a voltage-dependent channel, i.e., a peptide chain is not necessarily parallel to the normal to the bilayer. With liposomes, a situation where the amphipathic $3_{10}/\alpha$-helical trichogin GA IV would float on the bilayer, with the hydrophobic moieties (octanoyl group and Leu, Ile, and Lol side chains) buried into the membrane and the Gly-rich face exposed to the bulk water, cannot be discarded. Alternatively, an oblique disposition of the peptide, with the anchoring octanoyl chain deeply buried into the membrane, may also represent a plausible model.

The results described in this paper confirm unambiguously that the presence of a fatty acyl chain is essential for the membrane activity of the short lipopeptaibol trichogin GA IV [3]. In addition, they clearly indicate that moving the lipophilic moiety from the N$^\alpha$-blocking group to the side chain of the N-terminal extra-residue does not affect significantly the overall conformational properties or the membrane activity of the natural compound. In view of the rather flexible N-terminal segment and the excellent membrane activity of the [Ac-L-(αMe)Aun$^0$, L-Leu-OMe$^{11}$] analogue, it is premature to draw any definitive conclusion on the require-

 

ments for the orientation of the fatty acyl chain relative to the peptide backbone and on the mechanism of membrane permeability of trichogin GA IV. A study is currently underway in our laboratories aiming at discriminating among the different mechanistic possibilities discussed above by exploiting two series of synthetic analogues of trichogin GA IV, each designed to incorporate at selected positions of the peptide chain either a paramagnetic or a fluorescent amino acid residue. We are also examining the properties of trichogin GA IV and selected analogues under the conditions of voltage-controlled experiments, a prerequisite to probe the nature of a voltage-dependent channel.

## REFERENCES


1. C. Auvin-Guette, S. Rebuffat, Y. Prigent and B. Bodo (1992). Trichogin A IV, an 11-residue lipopeptaibol from *Trichoderma longibrachiatum*. *J. Am. Chem. Soc. 114*, 2170–2174.
2. C. Toniolo, C. Peggion, M. Crisma, F. Formaggio, X. Shui and D.S. Eggleston (1994). Structure determination of racemic trichogin A IV using centrosymmetric crystals. *Nature: Struct. Biol. 1*, 908–914.
3. C. Toniolo, M. Crisma, F. Formaggio, C. Peggion, V. Monaco, C. Goulard, S. Rebuffat and B. Bodo (1996). Effect of $N^{\alpha}$-acyl chain length on the membrane-modifying properties of synthetic analogs of the lipopeptaibol trichogin GA IV. *J. Am. Chem. Soc. 118*, 4952–4958.
4. V. Monaco, E. Locardi, F. Formaggio, M. Crisma, S. Mammi, E. Peggion, C. Toniolo, S. Rebuffat and B. Bodo (1998). Solution conformational analysis of amphiphilic helical, synthetic analogs of the lipopeptaibol trichogin GA IV. *J. Pept. Res.*, in press.
5. E. Locardi, S. Mammi, E. Peggion, V. Monaco, F. Formaggio, M. Crisma, C. Toniolo and J. Kamphuis (1997). Conformation of an analogue of the lipopeptaibol trichogin A IV containing the (αMe)Aun residue, in: *Peptides 1996*, R. Ramage and R. Epton, Eds, Mayflower Worldwide, Kingswindford, England, pp. 591–592.
6. W.J. McGahren and M. Goodman (1967). Synthesis of peptide oxazolones and related compounds. *Tetrahedron 23*, 2017–2030.
7. G. Valle, F. Formaggio, M. Crisma, G.M. Bonora, C. Toniolo, A. Bavoso, E. Benedetti, B. Di Blasio, V. Pavone and C. Pedone (1986). Linear oligopeptides. Part 147. Chemical and crystallographic study of the reaction between benzyloxycarbonyl chloride and α-aminoisobutyric acid. *J. Chem. Soc., Perkin Trans. 2*, 1371–1376.
8. M. El-Hajji, S. Rebuffat, T. Le Doan, G. Klein, M. Satre and B. Bodo (1989). Interaction of trichorzianines A and B with model membranes and with the ameba *Dictyostalium*. *Biochim. Biophys. Acta 978*, 97–104.
9. G. Drobny, A. Pines, S. Sinton, D.P. Weitekamp and D. Wemmer (1978). Fourier transform multiple quantum nuclear magnetic resonance. *Faraday Symp. Chem. Soc. 13*, 49–55.
10. G. Bodenhausen, R.L. Vold and R.R. Vold (1980). Multiple quantum spin-echo spectroscopy. *J. Magn. Reson. 37*, 93–106.
11. C. Griesinger, G. Otting, K. Wüthrich and R.R. Emst (1988). Clean TOCSY for $^{1}H$ spin system identification in macromolecules. *J. Am. Chem. Soc. 110*, 7870–7872.
12. G. Bodenhausen, H. Kogler and R.R. Ernst (1984). Selection of coherence-transfer pathways in NMR pulse experiments. *J. Magn. Reson. 58*, 370–388.
13. S. Macura, Y. Huang, D. Suter and R.R. Ernst (1981). Two-dimensional chemical exchange and cross-relaxation spectroscopy of coupled nuclear spin. *J. Magn. Reson. 43*, 259–281.
14. P. Güntert (1992). *DIANA Program Version 2.1*, *User's Manual and Instructions*, ETH, Zürich, Switzerland.
15. A.T. Brünger (1992). *X-PLOR Version 3.0 Manual*, Yale University, New Haven, CT.
16. W.H. Kruizinga, J. Bolster, R.M. Kellogg, J. Kamphuis, W.H.J. Boesten, E.M. Meijer and H.E. Shoemaker (1988). Synthesis of optically pure α-alkylated α-amino acids and a single-step method for enantiomeric excess determination. *J. Org. Chem. 53*, 1826–1827.
17. H.E. Shoemaker, W.H.J. Boesten, B. Kaptein, H.F.M. Hermes, T. Sonke, G.B. Broxterman, W.H.J. van den Tweel and J. Kamphuis (1992). Chemo-enzymatic synthesis of amino acids and derivatives. *Pure Appl. Chem. 64*, 1171–1175.
18. S. Beychok (1967). Circular dichroism of poly-α-amino acids and proteins, in: *Poly-α-Amino Acids*, G.D. Fasman, Ed., p. 293–337, Dekker, New York.
19. C. Toniolo, A. Polese, F. Formaggio, M. Crisma and J. Kamphuis (1996). Circular dichroism spectrum of a peptide $3_{10}$-helix. *J. Am. Chem. Soc. 188*, 2744–2745.
20. T. Miyazawa (1967). Infrared spectra and helical conformations, in: *Poly-α-Amino Acids*, G.D. Fasman, Ed., p. 69–103, Dekker, New York.
21. M. Palumbo, S. Da Rin, G.M. Bonora and C. Toniolo (1976). Infrared conformational analysis of homo-oligopeptides in the solid state and in solution. *Makromol. Chem. 177*, 1477–1492.
22. C. Toniolo, G.M. Bonora, V. Barone, A. Bavoso, E. Benedetti, B. Di Blasio, P. Grimaldi, F. Lelj, V. Pavone and C. Pedone (1985). Conformation of pleionomers of α-aminoisobutyric acid. *Macromolecules 18*, 895–902.
23. R. Nagaraj and P. Balaram (1981). Alamethicin, a transmembrane channel. *Acc. Chem. Res. 14*, 356–362.